

一种冷丝填充速度的 GABP 优化算法

张鹏贤^{1,2}, 李 浩^{1,2}, 张 杰¹

(1. 兰州理工大学 有色金属合金教育部重点实验室, 兰州 730050;

2. 兰州理工大学 甘肃省有色金属新材料省部共建国家重点实验室, 兰州 730050)

摘 要: 冷丝填充埋弧焊过程中, 冷丝填充量是决定焊缝组织和性能的主要参数。通过大量的工艺试验研究了冷丝填充量对微观组织和力学性能的影响, 利用焊接电弧热平衡规律建立了冷丝填充过程热量动态分配平衡方程, 推导出了计算冷丝填充速度的关系式。采用人工神经网络实现了焊接电流、电弧电压、焊接速度与冷丝填充速度的非线性映射关系。结果表明, 基于遗传算法的 BP 神经网络(BP neural network based on genetic algorithm, GABP) 优化算法实现了冷丝填充埋弧焊过程的自适应控制, 实际焊接冷丝填充速度与期望值之间的线性相关度达到 0.991 88, 表明该算法可以满足冷丝填充埋弧焊工艺及性能要求。

关键词: 冷丝填充埋弧焊; 热量动态分配; 遗传算法; BP 神经网络

中图分类号: TG409 **文献标识码:** A **文章编号:** 0253-360X(2012)12-0077-04



张鹏贤

0 序 言

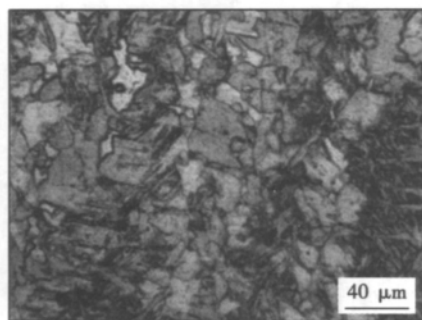
目前采用埋弧焊焊接高强度钢、控轧钢等热敏感性强的材料时, 由于高热输入导致熔池存在过多的热量, 致使母材受到过热损害, 其热影响区晶粒组织变得粗大, 易产生脆化等不利于接头性能的现象^[1]。合理控制熔池的能量分配可以减小过热对母材的损害。夏天东等人^[2]在埋弧焊过程中采用添加合金粉末的方法来平衡熔池热量的分配, 从而提高了熔敷速率, 减少了过热损害。但添加粉末实现起来相对复杂, 而且填充量不易控制。冷丝填充埋弧焊是在传统单丝埋弧焊过程中, 在熔池中插入一填充丝, 该填充丝无需供电电源, 故称冷丝。通过添加冷丝的方法来平衡熔池热量分配, 提高熔敷速率, 可减少对母材的过热损害^[3]。冷丝填充埋弧焊过程中, 合理的冷丝填充量是决定这种工艺方法应用效果的主要因素。若冷丝填充量过大, 致使熔深变浅, 熔合比降低, 堆高增大, 甚至出现母材未焊透、栽丝等现象。若冷丝填充量过小, 无法达到消耗熔池过多热量, 减小过热损害的目的, 这种工艺方法也就失去了存在的必要性。通过冷丝填充埋弧焊过程传热分析和试验研究, 确定了冷丝填充速度与焊接电流、

电弧电压、焊接速度等其它工艺参数的相关性, 探索了一种基于遗传算法的 BP 神经网络(GABP) 算法计算冷丝填充速度的方法。

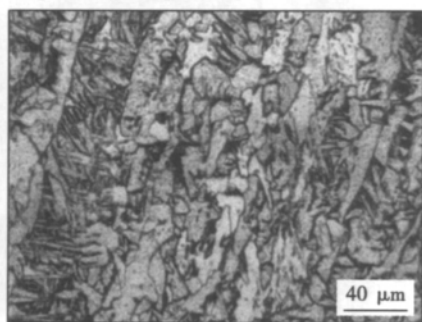
1 冷丝熔化热量平衡过程

冷丝填充埋弧焊过程中, 冷丝不断插入到熔池, 熔化的填充丝在熔池流体力学行为及电磁力的作用下被弥散在焊缝中, 与母材、熔滴过渡金属共同形成焊缝。图 1 为不加冷丝、填充与燃弧丝相同牌号的焊丝两种情况下获得的焊缝中心区域典型的金相显微组织。图 1a 中有较粗大的块状铁素体出现, 且个别部位观察到粗片状魏氏组织, 该焊缝组织多次测定的冲击吸收功分布在 65.2 ~ 72.5 J 范围内。而在图 1b 中观察到针状铁素体细小且多, 先共析铁素体晶粒细小且量少, 存在明显的柱状组织, 而填充冷丝下获得的焊缝其组织成分也是均匀分布的。该焊缝组织多次测定的冲击吸收功分布在 75.1 ~ 89.9 J 范围内, 其冲击韧性与不加冷丝时相比有明显提高。冷丝吸收熔池热量, 被熔化作为填充金属的同时, 致使熔池高温停留时间明显缩短, 这是其微观组织得以细化的主要原因。

液态高温熔池热源主要来自于电弧热和过渡到熔池的熔滴所包含的熔化潜热。从能量守恒角度讲, 冷丝填充埋弧焊过程中, 母材、燃弧丝、填充丝、焊剂熔化吸收的热量, 以及热交换过程损失的热量



(a) 不加冷丝时的焊缝组织



(b) 填充冷丝时的焊缝组织

图1 焊缝金相显微组织

Fig. 1 Microstructure of weld metal

和电弧产生的热处于动态平衡中. 将焊剂熔化和热交换过程损失的热量采用电弧热的熔化效率 η_m 来表达, 建立的冷丝填充埋弧焊过程热量平衡方程如式(1)所示, 即

$$v(A_m + A_e + A_l)\rho i_m = \eta_m UI \quad (1)$$

式中: v 表示焊接速度; A_e 、 A_l 、 A_m 分别为燃弧丝、冷丝和母材熔敷量对应的等效截面面积; ρ 为密度; i_m 表示母材和填充金属熔化的比热含量^[4]; U 和 I 分别表示电弧电压、焊接电流.

2 冷丝填充速度算法的建立

合理的控制冷丝填充量, 既能保证形成焊缝的母材熔敷率, 同时也可达到依靠冷丝熔敷率来消耗熔池过多热量、控制熔池温度场的目的. 冷丝填充量在冷丝直径选定的情况下主要取决于冷丝填充速度. 设冷丝熔化所需的热量为 q_1 , 则

$$q_1 = vA_l\rho i_m = \eta_m UI - v(A_m + A_e)\rho i_m \quad (2)$$

$$q_1 = v_1\pi\left(\frac{d}{2}\right)^2\rho c\Delta T \quad (3)$$

因此冷丝填充速度 v_1 为

$$v_1 = \frac{\eta_m UI - v(A_m + A_e)\rho i_m}{\pi\left(\frac{d}{2}\right)^2\rho c\Delta T} \quad (4)$$

式中: d 为冷丝的直径; ρ 和 c 分别为密度和比热容;

ΔT 为熔滴与加热的冷丝末端的温度差.

$$\text{设 } k_1 = \frac{\eta_m}{\pi\left(\frac{d}{2}\right)^2\rho c\Delta T} \quad k_2 = \frac{A_m + A_e}{\pi\left(\frac{d}{2}\right)^2} \text{ 则,}$$

$$v_1 = k_1 UI - k_2 v \quad (5)$$

k_1 、 k_2 由 η_m 、 A_m 、 A_e 、 ρ 、 c 和 d 等参数决定的, 其中 ρ 和 c 为常量, d 为冷丝直径, η_m 、 A_m 、 A_e 是随焊接过程不同而动态变化的. 因此冷丝填充埋弧焊过程是由多参数决定的非线性系统, 在给出了 U 、 I 和 v 的条件下, 由于 k_1 和 k_2 未知, 仍然无法直接计算出 v_1 . 在冷丝填充埋弧焊工艺试验过程中, 将满足合理的母材熔合比、焊缝显微组织及理想的强度和韧性作为评价指标条件下的焊缝作为合格焊缝, 其对应的 U 、 I 、 v 和 v_1 作为冷丝填充埋弧焊工艺参数. 图2和图3(图中 R 为线性相关度) 为冷丝填充速度 v_1 和其它工艺参数的关系曲线. 这两幅图表明, 在满足焊接接头性能要求下, 其冷丝填充速度 v_1 与 I 和 v 等其它工艺参数存在一定的单调线性关系.

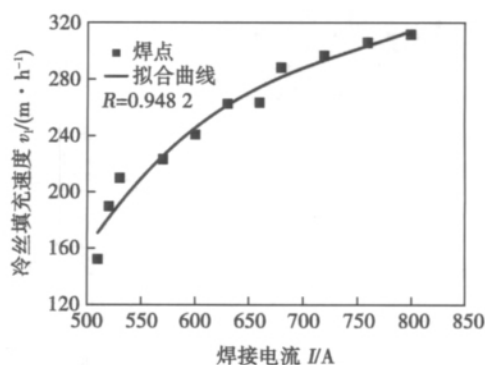


图2 冷丝填充速度与焊接电流的关系

Fig. 2 Relationship between filler rate of non-heated wire and welding current

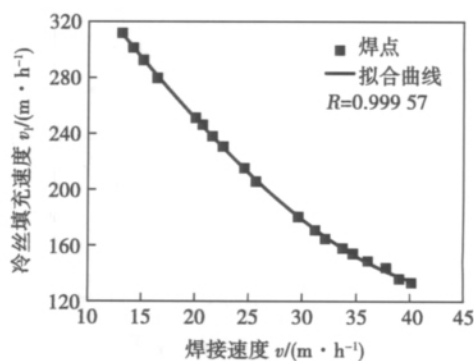


图3 冷丝填充速度与焊接速度的关系

Fig. 3 Relationship between filler rate of non-heated wire and welding speed

人工神经网络具有很强的并行处理、存储信息、

自适应、自组织、自学习、容错以及任意逼近非线性等优良特性,而且能较好地处理基于多因素、非线性和不确定性的问题^[5-6]。因此式(5)所表达的 v_1 与 U 、 I 、 v 间的映射关系可借助于人工神经网络算法实现。以焊接电流 I 、电弧电压 U 、焊接速度 v 作为网络输入向量,冷丝填充速度 v_1 作为网络输出,基于大量工艺试验获得的数据样本学习和训练,获得稳定的网络结构和权值。

3 GABP 算法的实现

BP 网络是目前人工神经网络应用中较成熟的网络,但 BP 神经网络存在收敛速度慢和容易陷入局部极值的缺点^[7]。而遗传算法具有智能式、渐进式的搜索、全局最优解、黑箱结构、通用性强和并行式算法等特点,它在整个操作过程中,同时控制着一个解群,而不是局限于一个点,这就大大提高了搜索效率,并避免陷入局部极值^[8-9]。针对冷丝填充埋弧焊过程,采用遗传算法结合 BP 神经网络建立了一种冷丝填充速度的优化算法。

基于遗传算法的 BP 神经网络(GABP),选取了三层的 BP 网络结构,输入节点 3 个,隐层节点 5 个,输出节点 1 个,把神经网络所有可能存在的连接权值和阈值作为个体的基因集,则种群中每个个体基因个数为 26,编码后作为种群的个体。根据个体得到 BP 神经网络的初始权值和阈值,用训练数据样本训练 BP 神经网络后预测系统输出,把预测输出和期望输出之间的误差绝对值和相对误差 E 作为个体适应度值 F 。遗传算法的选择操作采用轮盘赌法从种群中选择适应度好的个体组成新种群。交叉操作是从种群中选择两个个体,按一定概率交叉得到新个体。变异操作是从种群中随机选择一个个体,按一定概率变异得到新个体。

采用坡口为 V 形、板厚为 10 mm 的 16MnR,冷丝直径为 1.6 mm 进行冷丝填充埋弧自动对接焊接工艺试验。对焊后的焊缝从母材熔合比、显微组织、强度和韧性等方面进行评价,将所有合格焊缝对应的 U 、 I 、 v 和 v_1 作为数组,建立了用于神经网络训练和学习的数据样本。基于 Matlab 神经网络工具箱对建立的冷丝填充速度 GABP 算法进行了训练和仿真。在训练前采用 mapminmax 函数对数据进行归一化处理,把数据样本归一到 $[-1, 1]$ 。从数据样本中随机选择 40 组作为训练样本,20 组作为测试样本。其中 BP 算法的参数设置为:第一层传输函数选用 sigmoid 函数;第二层传输函数选用 purelin 函数;最大训练次数 1 000 次;学习率 0.01。遗传算法中种

群规模为 15,进化次数为 100 次,交叉概率为 0.4,变异概率为 0.2。两种算法的误差精度均为 0.000 01。对预测结果进行反归一化,获得的测试结果如图 4 和图 5 所示。圆点表示某测试样本下的算法仿真输出值,三角形符号代表该测试样本对应的冷丝填充速度目标值,两条拟合线的重合度反映了算法的收敛和泛化能力。

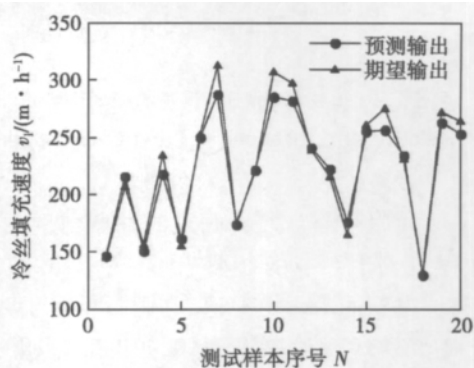


图 4 BP 算法测试结果

Fig. 4 Test results of BP algorithm

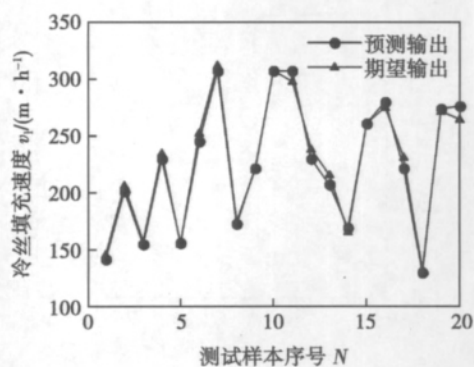


图 5 GABP 算法测试结果

Fig. 5 Test results of GABP algorithm

图 4 与图 5 对比表明,在同一测试样本下 GABP 算法的收敛速度和泛化能力优于 BP 算法。图 6 为测试过程两种算法的相对误差对比。在同一测试样本下,GABP 算法输出结果的相对误差显著小于 BP 算法的相对误差。计算获得的 GABP 算法均方误差为 $6.100\ 6 \times 10^{-4}$,而 BP 算法的均方误差为 2.1×10^{-3} ,这表明冷丝填充速度的 GABP 算法预测精度明显高于 BP 算法的。

采用材质仍为 16MnR 板的对接焊开展了冷丝填充埋弧焊工艺评定试验。试验表明,冷丝填充速度的 GABP 算法具有良好的泛化性和鲁棒性,板厚为 14.7 mm 对接焊缝,由算法确定的冷丝填充速度仍获得了满意的接头性能。实际焊接冷丝填充速度

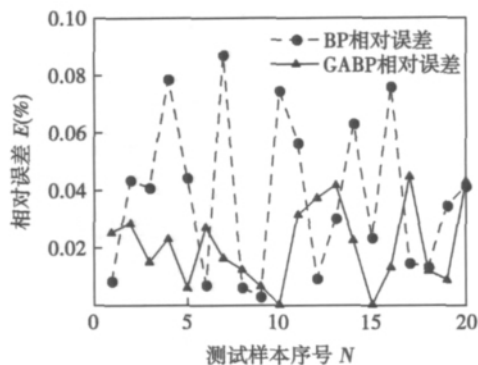


图 6 BP 算法与 GABP 算法的相对误差

Fig. 6 Relative error between BP and GABP algorithm

与由式(3)和焊后综合评价确定的期望值就有良好的接近程度,图 7 中的线性相关度 R 反映了由 GABP 算法得到的冷丝填充速度(目标值)与期望值的接近程度. 线性相关度 R 为 0.991 88 表明 GABP 算法可以满足冷丝填充埋弧焊工艺及性能要求.

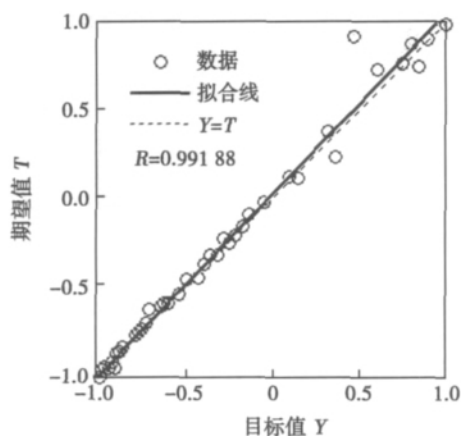


图 7 GABP 算法线性回归结果

Fig. 7 Linear regression results of GABP algorithm

4 结 论

(1) 通过对冷丝填充埋弧焊焊缝微观组织和力学性能的对比分析表明,冷丝填充量是决定冷丝填充埋弧焊工艺的主要参数. 基于大量工艺试验和冷丝填充过程传热分析,建立了冷丝填充埋弧焊过程热量动态分配平衡方程.

(2) 建立了以焊接电流、电弧电压和焊接速度为输入量,冷丝填充速度为输出量的冷丝填充速度 GABP 优化算法. 实际焊接结果表明,GABP 算法能够满足冷丝填充埋弧焊工艺及性能要求.

参考文献:

- [1] 高惠临,董玉华,王 荣,等. 管线钢焊接临界粗晶区局部脆化现象的研究[J]. 材料热处理学报,2001,22(2): 60-64.
Gao Huilin, Dong Yuhua, Wang Rong, *et al.* Study on local brittle zone phenomena of intercritically reheated coarse-grained heat-affected zone in pipeline steels [J]. Transactions of Metal Heat Treatment, 2001, 22(2): 60-64.
- [2] 夏天东,周 游,李浩河,等. 一种高效焊接技术-添加合金粉末埋弧焊[J]. 中国机械工程,1999,10(5): 580-582.
Xia Tiandong, Zhou You, Li Haohe, *et al.* A high efficient welding technique-submerged arc welding (SAW) with alloyed metal powders [J]. Chinese Journal of Mechanical Engineering, 1999, 10(5): 580-582.
- [3] 张鹏贤. 冷丝填充埋弧自动焊机数控系统的研制[J]. 电焊机,2003,33(10): 15-18.
Zhang Pengxian. Development of digital control system for submerged arc welder filled with non-heated wire [J]. Electric Welding Machine, 2003, 33(10): 15-18.
- [4] D. 拉达伊. 焊接热效应[M]. 北京: 机械工业出版社,1997.
- [5] 于秀萍,孙 华,赵希人,等. 基于人工神经网络的焊缝宽度预测[J]. 焊接学报,2005,26(5): 17-20.
Yu Xiuping, Sun Hua, Zhao Xiren, *et al.* Weld width prediction based on artificial neural network [J]. Transactions of the China Welding Institution, 2005, 26(5): 17-20.
- [6] 彭金宁,陈丙森,朱 平,等. 焊接工艺参数的神经网络智能设计[J]. 焊接学报,1998,19(1): 19-24.
Peng Jinning, Chen Bingchen, Zhu Ping, *et al.* Intelligent design of welding procedure parameters based on neural networks [J]. Transactions of the China Welding Institution, 1998, 19(1): 19-24.
- [7] Cook G E. Artificial neural networks applied to arc welding process modeling and control [J]. IEEE Transaction on Industry Application, 1990, 26(5): 824-830.
- [8] 董志波,魏艳红,占小红,等. 遗传算法与神经网络结合优化焊接接头力学性能预测模型[J]. 焊接学报,2007,28(12): 69-72.
Dong Zhibo, Wei Yanhong, Zhan Xiaohong, *et al.* Optimization of mechanical properties prediction models of welded joints combined neural network with genetic algorithm [J]. Transactions of the China Welding Institution, 2007, 28(12): 69-72.
- [9] Mok S L, Kwong C K, Lau W S. A hybrid neural network and genetic algorithm approach to the determination of initial process parameters for injection moulding [J]. The International Journal of Advanced Manufacturing Technology, 2001, 18: 404-409.

作者简介: 张鹏贤,男,1970 年出生,博士,教授. 主要从事焊接过程及其自动化、焊接质量控制等方面的研究. 发表论文 30 余篇.

Email: pengxizhang@163.com

A GABP optimized algorithm for filler rate of non-heated wire

ZHANG Pengxian^{1,2}, LI Hao^{1,2}, ZHANG Jie¹ (1. Key Laboratory of Non-ferrous Metal Alloys, The Ministry of Education, Lanzhou University of Technology, Lanzhou 730050, China; 2. State Key Laboratory of Gansu Advanced Non-ferrous Metal Materials, Lanzhou University of Technology, Lanzhou 730050, China). pp 77–80

Abstract: For the process of submerged arc welding filled with non-heated wire, the filler quantity of non-heated wire is one of the main parameters that affects the microstructure and mechanical properties of welded joints. First, through a lot of welding experiment, the effect of the filler quantity of non-heated wire on the microstructure and mechanical properties was investigated. On the basis of the heat balance law in welding process, the balance equation of heat dynamic distribution for the process of submerged arc welding filled with non-heated wire was established. Then the relational expression was formulated for the filler rate of non-heated wire. At last, the nonlinear mapping relationship between the welding current I , arc voltage U , welding speed v and filler rate of non-heated wire vl was realized based on artificial neural network. Experimental results showed that, the optimized algorithm of BP neural network based on genetic algorithm (GABP) can realize adaptive control for the process of submerged arc welding filled with non-heated wire. The linear correlation between filler rate of non-heated wire in actual welding process and the expectative output comes up to 0.991 88. This shows that the algorithm of GABP can meet requirement for welding process and properties.

Key words: submerged arc welding filled with non-heated wire; heat dynamic distribution; genetic algorithm; BP neural network

Simulation and experimental verification of double-pass welding temperature field for DP590 steel

XING Shuqing¹, HAO Fei², YAN Bo³, MA Yonglin¹ (1. School of Material and Metallurgy, Inner Mongolia University of Science and Technology, Baotou 014010, China; 2. Inspection and Maintenance Center, PetroChina LNG Jiangsu Co., Ltd, Nantong 226400, China; 3. Technology Center, Baotou Iron and Steel Co., Ltd, Baotou 014010, China). pp 81–84

Abstract: DP590 steel has been widely applied in the field of automobile industry. In present paper, the double-pass welding process in single-sided of CO₂ gas shielding was simulated by using parametric programming language and life-and-death cell technology. The numerical simulation results were compared with the experimental results obtained with the same preconditions. The results showed that the simulation result of temperature distribution within the sample is generally consistent with the measured temperature value. Compared with that of the first welding pass, the thermal cycling of the second pass has a greater impact on microstructure across the heat-affected zone. Because of the great influence of reheating temperature on the multi-pass welding process, it will be more advisable to maintain the temperature of the steel at around 200 °C at the beginning of second welding pass.

Key words: DP590 dual-phase steel; CO₂ gas shielded welding; numerical simulation; temperature field

Optimum design of magnesium alloy welding parameters with GTAW under magnetic field

SU Yunhai, JIANG Huanwen, WU Deguang, LIU Zhengjun (School of Material Science and Engineering, Shenyang University of Technology, Shenyang 110870, China). pp 85–88

Abstract: During the welding of AZ31 magnesium alloy plate by GTAW, AC longitudinal and conversion magnetic field were used. The magnetic field current and magnetic field frequency can be adjusted during welding process. Orthogonal experimental design was used to study the effect of parameters on the properties and microstructure of welded joint. The properties of tensile strength and hardness of welded joint were tested. The microstructure of magnesium welded joint was analyzed by metallographic microscope at the same time. The results show that the optimal properties of magnesium alloy welded joint are obtained when welding current is 80 A, magnetic field current is 2 A, and frequency is 20 Hz.

Key words: magnesium alloy; welding process under magnetic field; parameters optimum design

Factors affecting deformation induced martensitic transformation of SUS304 stainless steel

YANG Jianguo^{1,2}, CHEN Shuangjian^{1,3}, HUANG Nan¹, FANG Kun¹, YUAN Shijian¹, LIU Gang¹, HAN Cong⁵ (1. State Key Laboratory of Advanced Welding and Joining, Harbin Institute of Technology, Harbin 150001, China; 2. Institute of Process Equipment and Control Engineering, Zhejiang University of Technology, Hangzhou 310032, China; 3. Shanghai Institute of Applied Physics, Shanghai 201800, China). pp 89–92

Abstract: Tensile tests of SUS304 stainless steel specimens were performed with different strain rates at different temperatures. Moreover, the martensite induced by deformation was analyzed by ferrite measuring instrument, optical microscopy and XRD. Experimental results show that the transformation of martensite is closely related to uniformity of microstructure, strain rate and temperature. At room temperature, the amount of martensite induced by deformation increases with the increasing of tensile strain. For the tailor-welded tube endured 30% circumference strain in hydroforming process at temperature, the amount of martensite is higher in fusion zone than that in HAZ, and it is fewer in the base metal, i. e., the higher the uniformity, the less the amount of martensite transformation induced by deformation from austenite. The amount of martensite decreases with the increasing of testing temperature. Tensile tests at 275 °C indicated that martensite transformation induced by deformation can be restrained in the process of plastic deformation at this temperature, the volume fraction of martensite is almost 0 under such conditions.

Key words: deformation induced martensitic transformation; strain rate; microstructure heterogeneity; temperature; influencing factor

Forming process study of friction stir welding joint

ZHAO Huaxia, DONG Chunlin, LUAN Guohong (Beijing Aeronautical Manufacturing Technology Research Institute, Aviation Industry Corporation of China, Beijing 100024, China). pp 93–96